Nuclear Instruments and Methods in Physics Research A 785 (2015) 110–116

Contents lists available at ScienceDirect

Nuclear Instruments and Methods in Physics Research A

journal homepage: www.elsevier.com/locate/nima

Structural, mechanical and light yield characterisation of heat treated LYSO:Ce single crystals for medical imaging applications

P. Mengucci [a,*], G. André [b], E. Auffray [c], G. Barucca [a], C. Cecchi [d,1], R. Chipaux [e], A. Cousson [b], F. Davì [a], N. Di Vara [c], D. Rinaldi [a,1], E. Santecchia [a]

[a] Università Politecnica delle Marche, Via Brecce Bianche, 60131 Ancona, Italy
[b] Laboratoire Léon Brillouin, CEA-CNRS, CE-Saclay, 91191 Gif sur Yvette cedex, France
[c] Department PH-CMX CERN, Route de Meyrin, 1211 Geneva 23, Switzerland
[d] Dipartimento di Fisica e Geologia, Università di Perugia, Via A. Pascoli, 06123 Perugia, Italy
[e] CEA DSM/IRFU/SEDI, CE-Saclay, 91191 Gif sur Yvette cedex, France

ARTICLE INFO

Article history:
Received 8 October 2014
Received in revised form
21 February 2015
Accepted 26 February 2015
Available online 10 March 2015

Keywords:
Scintillating crystals
Electron microscopy
X ray diffraction
Neutron diffraction
Light yield
Mechanical characterisation.

ABSTRACT

Five single crystals of cerium-doped lutetium yttrium oxyorthosilicate (LYSO:Ce) grown by the Czochralski method were submitted to structural characterisation by X-ray (XRD) and neutron (ND) diffraction, scanning (SEM) and transmission (TEM) electron microscopy and energy dispersive microanalysis (EDS). The Ultimate Tensile Strength (UTS), the Young Modulus (YM) and the Light Yield (LY) of the samples were also measured in order to correlate the mechanical and the optical behaviour of the crystals with the characteristics of their microstructure. Two of the samples analysed were also heat treated at 300 °C for 10 h to evidence possible variations induced by the temperature in the optical and mechanical response of the crystals. Results showed that the mean compositional variations evidenced by the structural analyses do not affect the mechanical and optical behaviour of the samples. On the contrary, the thermal treatment could induce the formation of coherent spherical particles (size 10 to 15 nm), not uniformly distributed inside the sample, that strongly reduce the UTS and YM values, but it does not affect the optical response of the crystal. This latter result was attributed to the low value of the heating temperature (300 °C) that is not sufficiently high to induce annealing of the oxygen vacancies traps that are responsible of the deterioration of the scintillation properties of the LYSO:Ce crystals.

This study was carried out in the framework of the Crystal Clear Collaboration (CCC).

1. Introduction

Cerium-doped lutetium yttrium oxyorthosilicate crystal ($Lu_{2(1-x)}Y_{2x}SiO_5$:Ce namely LYSO:Ce) has attracted the attention of the researchers since the early 1990s [1] due to its scintillation properties that are of interest to the fields of the high energy physics [2–7] and the nuclear medicine [8–11]. For medical applications, it is only since the early 2000 that LYSO:Ce started to be considered as a valid alternative to the BGO for Positron Emission Tomography (PET) due to its high density, high light yield, fast decay time and good coincidence resolving time [11,12]. This latter property makes the LYSO:Ce crystal particularly suitable for time-of-flight applications (TOF-PET) [13].

From a structural point of view, lutetium yttrium oxyorthosilicate (LYSO) is a solid solution of the Lu_2SiO_5 (LSO) and Y_2SiO_5 (YSO) silicates with structural parameters and physical properties depending on the relative concentration of the two silicates, so much that the concentration of the LYSO solid solution is commonly indicated by the Y/Lu ratio [14].

In the past decades, the structure of LYSO single crystals considered as a solid solution of LSO and YSO was extensively studied and its crystallography is now well established [14–17]. Moreover, due to the high applicative interest, the Ce-doped LYSO (LYSO:Ce) single crystals are still under study in order to better understand the correlation between the chemical composition of the crystals and their structural and scintillation properties [18,19].

A number of papers can be found in literature reporting on the scintillation performances of LYSO:Ce crystals and many authors have addressed the problem how to improve the scintillation response of such crystals [20–25]. The details of the scintillation mechanism have been also deeply investigated with special regard to the possible crystallographic or compositional defects responsible of the scintillation losses [22,26,27]. In particular, it was shown that the deterioration of the scintillation performances must be ascribed to the presence of optically active traps inside the

* Correspondence to: Dipartimento SIMAU, Università Politecnica delle Marche, 60131 Ancona, Italy.
E-mail address: p.mengucci@univpm.it (P. Mengucci).
[1] INFN section of Perugia.

http://dx.doi.org/10.1016/j.nima.2015.02.061
0168-9002/

crystal lattice [22–27]. Thermoluminescence (TL) measurements carried out in conjunction with thermal annealing experiments performed in reducing or oxidising atmosphere showed that traps are related to oxygen vacancies [21,22,28,29]. Moreover, Blahuta et al. [22] on the basis of their experimental evidences concluded that the oxygen vacancies are located close to the dopant ions (Ce^{3+}) within few interatomic distances, because the trapping mechanism involves electron tunnelling. An effective way to reduce the number of traps and consequently to improve the scintillation response of the scintillating crystals was demonstrated to be thermal annealing at high temperature (1100–1500 °C) for time ranging from 10 to 48 h [22,30]. Recently, Blahuta et al. [26] also showed how the enhanced scintillation properties in LYSO:Ce,Mg and LYSO:Ce,Ca single crystals depend on the Ce^{4+} content in co-doped crystals [31–34].

In spite of the large number of papers dealing with the problems related to the LYSO:Ce single crystals that still limit their massive applications in the field of the medical imaging systems, a very limited number of papers appeared in literature discussing the mechanical properties of the LYSO:Ce crystals, even though the implementation of the imaging systems based on the LYSO:Ce crystals on an industrial scale requires a complete knowledge of the scintillating behaviour as well as the mechanical properties of the crystals.

To our knowledge, up to now only Scalise et al. [35] reported on the experimental measurements of the Ultimate Tensile Strength and Young Modulus of LYSO:Ce single crystals while Davì and Rinaldi [36] proposed a theoretical model based on the continuum mechanics able to justify the optical and mechanical behaviour of the crystals. Furthermore, always to our knowledge, any study that reports on the possible correlations of the structural characteristics of the crystals with their mechanical properties and scintillation behaviour, is not present in literature, up to now.

In this paper, for the first time, the correlation between the microstructure and the Ultimate Tensile Strength (UTS) and Young Modulus (YM) measured on LYSO:Ce single crystals is proposed. Furthermore, the scintillation properties of the crystals are interpreted in function of their average composition in accordance to the scintillation mechanisms proposed in literature [21–30].

It must be stressed that this study was carried out in the framework of the Crystal Clear Collaboration (CCC) to which belong a number of research groups with complementary expertise. The samples analysed in this work are five out of the 12 samples mechanically tested by Scalise et al. [35]. Two samples among the five investigated, were submitted to a thermal annealing process at 300 °C for 10 h in order to evidence possible variations in the structural, mechanical and scintillation properties as a consequence of the thermal treatment.

The structure characterisation of the crystals was carried out by X-Ray Diffraction (XRD), Neutron Diffraction (ND), Scanning Electron Microscopy (SEM), Transmission Electron Microscopy (TEM) and Energy Dispersive Spectroscopy (EDS). The Light Yield (LY) measurements were performed at CERN by the PH-CMX group.

2. Experimental methods

Cerium-doped lutetium yttrium oxyorthosilicate crystals ($Lu_{2(1-x)}Y_{2x}SiO_5$:Ce namely LYSO:Ce) were grown from the melt with a nominal composition $x=0.1$ ($Lu_{1.8}Y_{0.2}SiO_5$:Ce) by using the Czochralski method. The Ce concentration in the melt remains below 1 at%.

From the same raw billet, parallelepiped crystals with a square section of 0.5×0.5 cm^2 and a length of 10 cm were cut by a wire saw. The crystals size was set in order to fit the four-point bending device used for the mechanical tests, described in the paper by Scalise et al. [35]. Each crystal cut from the billet has the optical axis, that is directed along the [0 1 0] crystallographic direction of the LYSO:Ce crystal, coincident with the parallelepiped axis. After the cutting process, all the surfaces of each parallelepiped crystal were carefully polished. At the end of the complete production process the crystal appears colourless and perfectly transparent without any visible inclusion.

Five crystals produced as reported above were submitted to mechanical testing, structural characterisation and light yield measurements. Furthermore, two out of the five samples were also subjected to a thermal treatment at 300 °C for 10 h. The details of the thermal treatment and the detailed results of the mechanical tests have been reported and discussed in the paper by Scalise et al. [35]. It must be underlined that the five crystals analysed in this study are exactly the same samples (reported also with the same name) investigated in the paper by Scalise et al. [35].

In order to understand the reason of the low annealing temperature (300 °C) adopted in this study, it must be stressed that annealing temperatures in the range 300–800 K were used to relieve defects after high energy irradiation, for example, in LiF single crystals [37,38]. In the cited papers, authors show that the thermal treatments performed at temperatures in the range 300–800 K are able to relieve the crystallographic defects formed during irradiation as well as to modify the mechanical properties of the crystals. To our knowledge, annealing temperatures as low as 300 °C, corresponding to about 600 K, were never used for thermal treating LYSO:Ce scintillating crystals. Furthermore, even the mechanical properties of LYSO:Ce single crystals were poorly investigated in the past. Therefore, the main idea at the basis of this study was to check whether a thermal treatment carried out at low temperature (300 °C), similar to the annealing treatments used for LiF crystals, is capable to induce any variation in the structural, mechanical or optical properties of LYSO:Ce unirradiated crystals. The Ultimate Tensile Strength (UTS) and Young Modulus (YM) of the five LYSO:Ce single crystals considered in this study were deeply investigated by Scalise et al. [35].

In this paper we focus our attention mainly on the structural and light yield measurements although a correlation between the mechanical behaviour and the samples microstructure will be proposed.

The structural characterisation of the samples was carried out by X-Ray (XRD) and Neutron (ND) Diffraction techniques, Scanning Electron Microscopy (SEM) and Transmission Electron Microscopy (TEM) observations and Energy Dispersive Spectroscopy (EDS) microanalysis.

In order to obtain easily handle samples to submit to the structural characterisation techniques mentioned above, small sections about 1 mm thick were cut from the parallelepiped crystal by a low speed diamond blade making sure to keep the opposite faces as parallel as possible. The damage induced by the cutting procedure was removed by grinding papers.

XRD investigations were performed by a Bruker D8 Advance diffractometer in Bragg–Brentano geometry by using the Cu-Kα radiation. Spectra refinement and Rietveld analysis were carried out by the FullProf code [39]. The XRD measurements were conducted on samples manually reduced to powder into a mortar.

Neutron diffraction experiments were performed at the Laboratoire Léon Brillouin, on a fragment of a monocrystal on the single crystal diffractometer 5C2 located at the hot source of the Orphee reactor [with $\lambda=0.0832$ nm], and on manually powdered sample issued from the same batch on the powder diffractometer G41 with $\lambda=0.242$ nm.

A Zeiss SUPRA40 field emission scanning electron microscope equipped with a Bruker Quantax Z200 EDS microanalysis was used to analyse both the surface microstructure and the mean composition of the crystals. SEM observations were carried out by using both secondary electrons (SE) to evidence surface topography, and

backscattered electron (BSE) to observe compositional variations eventually present in the sample. In order to perform an adequate statistics of the sample mean composition, EDS analyses were performed by taking 20 acquisitions from different areas ($\sim 100 \times 100\ \mu m^2$) of the sample. The penetration depth at an electron beam energy of 10 keV, estimated by a Monte Carlo simulation performed by using the CASINO programme [40] on the basis of the LYSO:Ce composition, is about 0.9 μm.

Transmission electron microscopy (TEM) observations were performed by a Philips (FEI) CM200 microscope operating at 200 kV and equipped with an EDAX Genesis EDS microanalysis. For TEM observations, samples were mechanically thinned by grinding papers and polished by diamond pastes. TEM disks with a diameter of 3 mm were cut by an ultrasonic cutter (Gatan model 601) and then the central part of each disk was further mechanically thinned by a dimple grinder (Gatan model 656). The final thinning of the disks was carried out by an ion beam system (Gatan PIPS model 695) using Ar ions at 5 kV.

Light yield measurements were performed at CERN, PH-CMX group by using an experimental setup equipped with a Photo Multiplier Tube Photonis XP2020Q and a Caen Digitizer (ref.: DT5720). The crystals have been characterised with a Caesium-137 source. In order to obtain comparable light emission values with respect to the attenuation of scintillation light, the crystals were cut in a final size of $0.5 \times 0.5 \times 2.5\ cm^3$. The crystals, cut in the just mentioned final size, were optically coupled with optical grease to the photocathode and fully wrapped in Teflon. Samples were measured in vertical position along the 2.5 cm wide crystal side. In order to get the quantum efficiency, the emission spectrum of the crystals was convoluted with the quantum efficiency curve previously measured for the corresponding tube.

3. Results and discussion

The results of the mechanical tests, in terms of Ultimate Tensile Stress (UTS) and Young Modulus (YM), are reported in Table 1. In particular, the analysed samples are listed in Table 1 in ascending order of the UTS and YM values to facilitate the exposure of the results that follow.

It is worth noting that the experimental error due to the instrumental uncertainty in the UTS values reported in Table 1 is $\Delta\sigma_{UTS} = \pm 3$ MPa [35].

From Table 1 it is evident that only samples 1 and 6 were submitted to the thermal annealing before the mechanical tests while samples 8, 10 and 11 were mechanically tested without any further treatment. The details of the procedure adopted for measuring the mechanical properties of the samples have been reported in the paper by Scalise et al. [35].

Table 1 shows that sample 11, not heat treated, has the highest values of UTS and YM. On the other side, the lowest values of UTS and YM were obtained for sample 6 that was subjected to thermal annealing. Furthermore, samples 8 and 10 (not annealed) show very similar mechanical behaviour, while sample 1 (annealed) exhibits mechanical properties intermediate between those of the samples 8 and 10 (not annealed) and that of the sample 11 (not annealed). Therefore, at this stage it is difficult to postulate possible correlations between the mechanical behaviour and the thermal treatment of the crystals given the small number of samples tested and the lack of an appropriate model. However, the UTS and YM values of sample 6 (annealed) seem to be anomalous if compared to the UTS and YM values of the other samples, suggesting the worst mechanical response of sample 6 with respect to the other samples, regardless the thermal treatment undergone.

Table 1
Ultimate Tensile Strength (UTS) and Young Modulus values of the LYSO:Ce crystals analysed in this work. The details of the procedure used to measure the UTS and YM values have been reported elsewhere [35].

Sample	UTS (MPa)	YM (MPa)	Annealing
#6	68	129	Yes
#8	78	174	No
#10	79	174	No
#1	94	182	Yes
#11	114	186	No

On the basis of these considerations, we focused our attention on the possible structural differences between sample 6 and all the other samples, able to justify the observed differences in the mechanical behaviour reported in Table 1.

The crystallographic structure of the samples was investigated by X-ray diffraction (XRD) and neutron diffraction (ND) analyses. The XRD patterns of all the analysed samples reduced to powder are very similar and the Rietveld refinement provided comparable results. For this reason, in Fig. 1 is reported the XRD pattern of sample 10 that is considered representative of the XRD pattern of all the samples analysed. In Fig. 1 the solid squares are the experimental data points, the superimposed continuous line is the Rietveld fitting while the continuous line below the pattern represents the residuals. The Rietveld refining provided a monoclinic crystallographic structure, space group C2/C.

The ND analysis confirmed the monoclinic crystallographic structure with a C2/C space group. Powder diffraction with the G41 diffractometer gives the more precise values of lattice parameters: $a = 14.245(2)$ Å, $b = 6.635(1)$ Å, $c = 10.242(1)$ Å, $\beta = 122.188(10)^\circ$ and a crystal cell volume $V = 819.26(18)$ Å^3, whereas the 5C2 instrument provides less resolved ones (respectively $a = 14.21(10)$ Å, $b = 6.61(10)$ Å, $c = 10.24(10)$ Å, and $\beta = 122.11(10)^\circ$) but gives the atomic positions reported in Table 2.

These values are in agreement with the values already reported in literature for similar compositions [14,15,18,19,41]. Attempts to refine the difference in occupancy on the rare-earth sites by lutetium, yttrium and cerium were unsuccessful due to the low contrast induced by the proximity of the respective Fermi's lengths of these atoms (7.21 fm for Lu, 7.75 fm for Y, 4.84 for Ce, but only ~1% content).

SEM observations of the samples surface morphology show a smooth surface free of macroscopic defects for all the analysed samples. Furthermore, the SEM observations of the samples carried

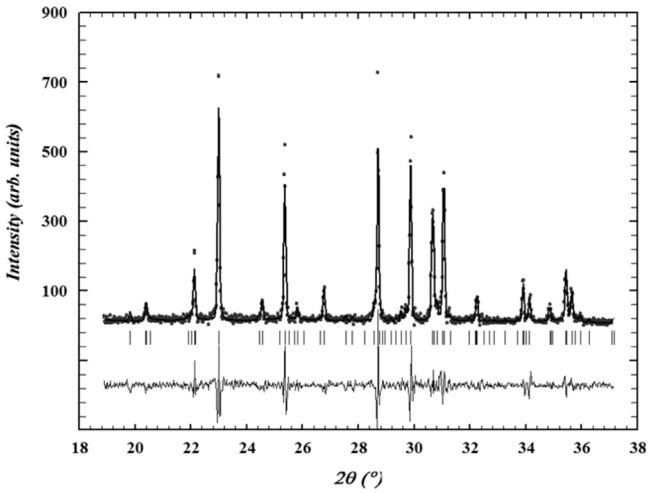

Fig. 1. X-ray diffraction (XRD) pattern of the crystals manually reduced to powder. Solid squares – data points, continuous line – Rietveld refining, continuous line below the pattern – residuals.

Table 2
Atomic positions in LYSO measured by single crystal neutron diffraction.

Ion and crystallographic site	*x*	*y*	*z*
Lu^{3+} 1	0.53747(3)	0.75600(3)	0.46697(3)
Lu^{3+} 2	0.64089(3)	0.87722(3)	0.83632(3)
Si^{4+} 1	0.31783(6)	0.59092(11)	0.19294(8)
O^{2-} 1	0.41116(5)	0.50554(10)	0.36156(7)
O^{2-} 2	0.61982(5)	0.78838(9)	0.32350(7)
O^{2-} 3	0.70249(5)	0.85154(10)	0.67685(7)
O^{2-} 4	0.70162(5)	0.57106(10)	0.93706(7)
O^{2-} 5	0.48219(5)	0.90358(9)	0.60245(6)

Table 3
Element concentration obtained from the EDS analysis performed in conjunction with the SEM observations.

Sample	Lu (at%)	Y (at%)	Ce (at%)	Annealing
#6	23.6	2.5	0.3	Yes
#8	22.8	2.6	0.6	No
#10	25.0	3.0	0.2	No
#1	23.0	2.5	0.5	Yes
#11	28.9	2.3	< 0.1	No
Nominal	22.5	2.5	< 1.0	

out by the Back Scattered Electron (BSE) detector signal did not evidence any compositional contrast in the images of the samples, suggesting that compounds formation and/or elements segregation did not take place. The absence of any compound formed during the crystal growth as well as the absence of sample regions inside which elements with different atomic numbers tend to segregate agrees with the conclusions of Ding et al. [18] on the nature of the LYSO solid solution. In fact, Ding et al. [18] say that since the LSO–YSO system is an infinite solid solution system, Lu and Y in LYSO can vary in a wide range without forming any compound. Therefore, the crystal $(Lu_{1-x}Y_x)_2SiO_5$:Ce (LYSO:Ce) can be grown from the melt with an arbitrary value of x from 0 to 100, in at% [18].

In conjunction with the SEM observations, samples were submitted to EDS analysis performed on large areas ($\sim 100 \times 100\ \mu m^2$) of the sample. At least 20 different areas for each sample were investigated in order to increase the statistics of the results that are summarised in Table 3 for Lu, Y and Ce, expressed in atomic percentage (at%). The experimental error associated to the element concentration reported in Table 3 was estimated to be ± 0.1 at%.

It is necessary to point out that, as an analytical technique, EDS has a very low sensitivity and consequently a low reliability to low atomic number elements (carbon, oxygen). This is the reason why in Table 3 we report only the atomic content, experimentally obtained by EDS analysis, of the higher atomic number elements (Lu, Y, Ce). Furthermore, in order to facilitate the comparison and the interpretation of the results, in Table 3 samples are listed in the same order of Table 1, i.e. according to the increasing value of YM and UTS.

The values listed in Table 3 represent the average values obtained from the 20 measurements performed on each sample and they must be compared to the nominal values, reported in the last row of Table 3, on the basis of the nominal composition $Lu_{1.8}Y_{0.2}SiO_5$:Ce of the LYSO:Ce crystal, that corresponds to $x=0.1$ in the $(Lu_{1-x}Y_x)_2SiO_5$:Ce chemical formula. Table 3 also shows that, in agreement with the nominal composition reported in the experimental session above, the Ce content remains below 1 (at%). Furthermore, it is evident that the mean composition of the LYSO:Ce crystals show a wide range of variability, regardless the annealing treatment.

From Table 3 it is also possible to note that, although the annealed samples (6 and 1) have very similar compositions close to the nominal one, their mechanical properties result sensibly different (Table 1). On the other hand, samples 8 and 10 that exhibit a similar mechanical behaviour (Table 1) have a sensibly different mean chemical composition (Table 3). Therefore, it is evident that the different mechanical behaviour of the samples studied in this work cannot be correlated to the variations of their mean chemical composition on areas of the sample as large as those investigated by the EDS technique.

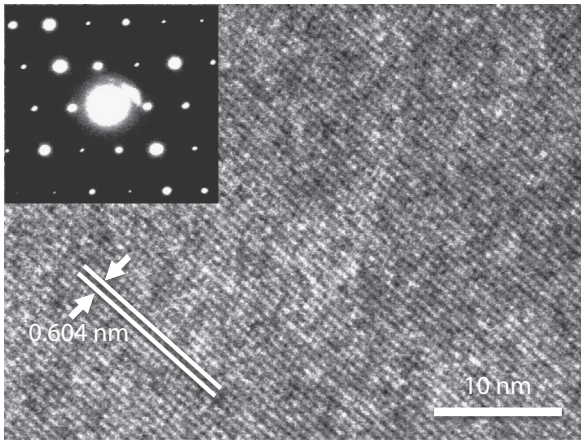

Fig. 2. High resolution transmission electron microscopy (HRTEM) image and corresponding selected area electron diffraction (SAED) pattern taken in ⟨010⟩ zone axis orientation.

In order to study in detail the inner structure of the samples on small areas and to evidence possible structure variations, TEM observations were performed. In the transmission electron microscope the crystallographic characteristics of the samples were also investigated by selected area electron diffraction (SAED) analyses and high resolution TEM (HRTEM) observations. Fig. 2 shows the HRTEM image of the sample 8 taken in ⟨010⟩ zone axis orientation with the corresponding SAED pattern in the inset. The indexation of the SAED pattern allowed to confirm the crystallographic structure of the LYSO:Ce crystal that results to be monoclinic with the lattice parameters in agreement with those obtained from the XRD and ND measurements reported above.

The lattice spacing of the planes visible in Fig. 2 is 0.604 nm corresponding to the (200) lattice planes of the monoclinic crystal. From the HRTEM image and the SAED pattern in Fig. 2 is possible to conclude on the absence of crystallographic defects and secondary phases in the observed sample. Similar results were also obtained for samples 1, 10 and 11. Therefore, all these samples (1, 8, 10 and 11) have the same crystallographic structure and are free of lattice defects and secondary phases, regardless the thermal treatment undergone.

A completely different microstructure was observed for sample 6. In fact, although its crystallographic structure is monoclinic with the same lattice parameters measured in the other samples, sample 6 shows a non-homogeneous distribution of crystallographic defects. Fig. 3 reports the TEM bright field images of two different areas of sample 6, taken at the same magnification. In Fig. 3a the density of defects is particularly high while in Fig. 3b it is sensibly lower. Similar results were obtained on the different areas analysed, indicating a non-homogeneous distribution of defects throughout the sample.

As far as the nature of the crystallographic defects is concerned, it is possible to infer some information from the experimental conditions used to obtain the TEM bright field images. The two images reported in Fig. 3 were taken in two beam condition ($g=(002)$) with the sample oriented close to the ⟨0 10⟩ zone axis of the monoclinic lattice. Under this condition the defects show a typical "coffee bean" contrast, constituted of a bright central line ("line of no contrast") surrounded by two lateral dark lobes (Fig. 3). As

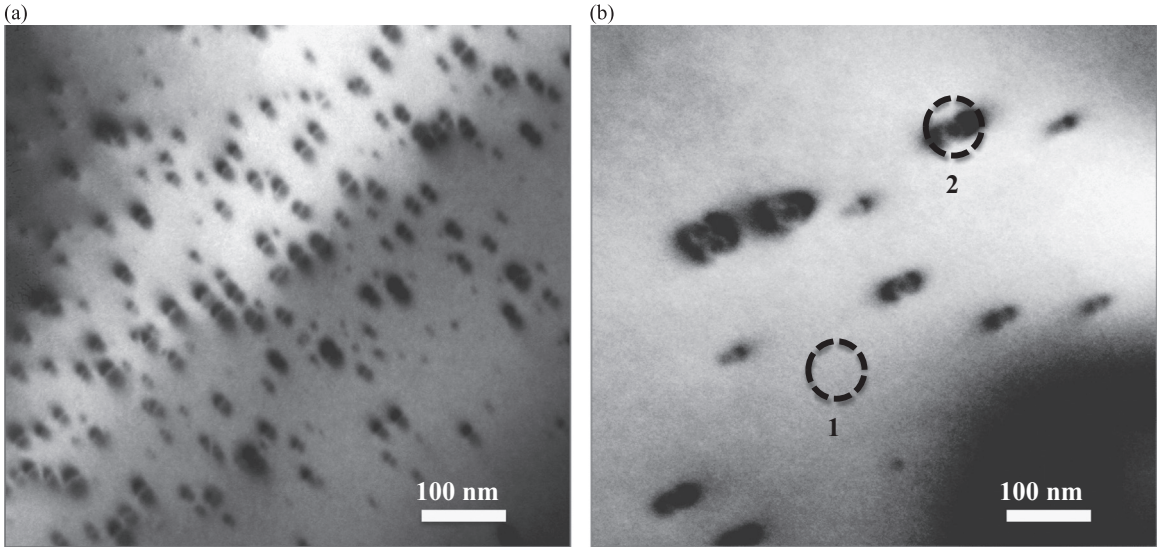

Fig. 3. Transmission electron microscopy (TEM) images of sample 6. (a) Area of the sample with a high density of the coherent lattice defects, (b) area of the sample with a lower density of defects. Dashed circles indicates the two zone on which EDS analyses were performed: (1) Zone 1 – matrix, (2) Zone 2 – lattice defect.

known from literature, this type of contrast is due to the lattice displacements near a particle showing spherically symmetrical strains [42]. The dimension of the dark lobes depends on both the value of the lattice strain around the particle and the observation conditions, i.e. the excited *g* in the two beam condition mode [42]. Therefore, from the above considerations, we conclude that the lattice defects evidenced by the TEM observations are coherent spherical precipitates non-homogeneously distributed inside the sample. An estimation of the coherent particle size provided values ranging from 10 nm to 15 nm.

It is worth to note that a coherent lattice defect have the same crystallographic structure of the matrix within which it is embedded. Typically, such defects are due to the displacement of few atoms from the lattice sites that do not alter the crystallographic structure of the crystal. In our case, the coherent spherical particles observed in sample 6 have the same crystallographic structure of the LYSO:Ce crystal.

Sample 6 was also submitted to EDS analysis during the TEM observations with the aim to evidence possible compositional variations between the coherent spherical particles and the matrix. Several measurements were performed on different areas of the sample that gave almost always the same results, except for the Ce content. Hence, we report here the results of the EDS microanalysis obtained on two different areas. In each area we analysed two different zones like those circled in Fig. 3b. The EDS microanalysis was performed with the electron beam of the transmission microscope focused on each zone and the two spectra were collected separately. The zone labelled "1" in Fig. 3b, free of precipitates, corresponds to the matrix while the zone "2" was centred on a particle. Of course, due to the small size of the precipitates, the dimension of the analysed area is always larger than the single precipitate. This means that the results obtained from the EDS must be considered as a rough indication of possible variations in composition between the matrix (zone 1 in Fig. 3b) and the particle (zone 2 in Fig. 3b). The results of the EDS analysis obtained from two different areas of sample 6 are reported in Table 4.

The experimental error of the concentration values in Table 4 is ± 0.1 at%. The two different areas of the sample are named "A1" and "A2", inside each area EDS analysis was performed on the matrix (zone 1 – Z1) and on the spherical particle (zone 2 – Z2).

Table 4 shows in both cases an increase in the content of Lu and Y in the precipitate (zone 2) with respect to the matrix (zone 1).

Table 4
Results of the EDS analysis performed on the matrix and on a single coherent particle in two different areas of the sample 6.

Area/zone	Lu (at%)	Y (at%)	Ce (at%)	Si (at%)
A1/Z1 – Matrix	10.2	0.9	0.4	88.5
A1/Z2 – Particle	11.6	1.1	0.2	87.1
A2/Z1 – Matrix	9.9	0.9	0.3	88.9
A2/Z2 – Particle	10.7	1.1	0.5	87.7

Table 5
Results of the light yield (LY) measurements.

Sample	LY (ph/MeV)	Annealing
#6	16300	Yes
#8	16100	No
#10	16500	No
#1	16450	Yes
#11	16600	No

On the contrary, the Ce content does not seem to follow any particular trend because it decreases in the precipitate of area "A1" and increases in the precipitate of area "A2" (Table 4). However, although this latter result could be ascribed to a non-homogeneous dispersion of Ce inside the sample, it must be considered that the amount of Ce is at the limit of the EDS sensitivity.

All the analysed samples were also submitted to light yield (LY) measurements to investigate possible modifications of the optical response as a consequence of the microstructure variations. The results of the LY measurements are reported in Table 5, where the samples are listed according to the increasing value of YM and UTS to facilitate the comparison with Tables 1 and 3.

Although the experimental LY values obtained from the investigated LYSO:Ce crystals (Table 5) are lower than the LY values commonly reported in literature (≈ 30000 ph/MeV) for LYSO:Ce, it must be considered that our samples were measured in vertical position along the widest crystal side (2.5 cm). The high LY values of 30,000 ph/MeV commonly reported in literature for LYSO:Ce crystals were obtained measuring small sized crystals, typically about 0.5 cm wide [25]. Therefore, absorption, that plays an important role in the final LY value, must be taken into account

when LY measurements taken from different sized crystals are compared.

The measured LY values for all the analysed samples are very similar regardless the thermal treatment undergone and the sample microstructure, as shown in Table 5. Indeed, this is a very surprising result especially if one considers that sample 6 that shows the presence of spherical coherent lattice defects, not seen in the other samples, has the same scintillation behaviour of the other samples. Anyhow, the LY results reported in Table 5 demonstrate that the extended crystallographic defects (coherent spherical particles) with an average size around 10 nm observed in the sample 6 do not affect the scintillation properties of the crystal.

It is well known that the optically active traps capable of sensibly reducing the scintillation performances of the LYSO:Ce crystals are the oxygen vacancies located within few interatomic distances from the Ce ions [22–27]. Since the dopant atom (Ce) is quite uniformly distributed in the lattice of the LYSO crystal, it is reasonable to assume that also the optical traps have a similar distribution in the crystal lattice. Thus, the scintillation losses occur at the oxygen traps distributed in the entire volume of the crystal, suggesting a general effect dependent on the crystal volume [22–27]. On the other hand, the crystallographic defects (coherent spherical particles) observed in the sample 6 have a mean size ($\sim$10 nm) about 100 times larger than the distances within which the electron trapping due to oxygen vacancies occurs. Moreover, these coherent particles in the sample 6 were observed to be concentrated in large areas of the sample, but not uniformly distributed throughout the volume. The combination of these two facts, the large size of the precipitates and their non-uniform distribution, invalidates the possibility of sensible scintillation losses associated to the coherent precipitates, leading to a LY behaviour of the sample 6 comparable to the LY behaviour of all other samples (Table 5).

Furthermore, if the scintillation losses must be entirely ascribed to the oxygen vacancies, as reported in literature [22–27], the almost equal LY values measured in our samples (Table 5) suggest a substantial uniform density of oxygen vacancies in all the analysed samples, included those heat-treated. This latter result allows concluding that the heat treatment at 300 °C for 10 h performed on the samples 1 and 6 [35] has no annealing effect on the oxygen vacancies. Concerning this point, it is worth to note that the annealing treatments reported in literature to improve the scintillation properties of the LYSO crystals were carried out at higher temperatures (1100–1500 °C) for time ranging from 10 to 48 h [22,30].

On the other hand, sample 6 shows the lowest values of UTS and YM, as shown in Table 1. This mechanical behaviour can be reasonably correlated, in absence of an adequate model and further investigation in progress, to the presence of the coherent spherical precipitates probably formed during the heat treatment. Therefore, although the heat treatment performed on samples 1 and 6 is not able to induce annealing of the oxygen vacancy traps, it could however induce the formation of extended lattice defects (spherical coherent particles) that affect the mechanical properties of the samples.

4. Conclusions

Five samples of Cerium-doped lutetium yttrium oxyorthosilicate crystals (namely LYSO:Ce) grown by the Czochralski method with nominal composition ($Lu_{1.8}Y_{0.2}SiO_5$:Ce) were investigated by X-Ray Diffraction (XRD), Neutron Diffraction (ND), Scanning Electron Microscopy (SEM), Transmission Electron Microscopy (TEM), Energy Dispersive Spectroscopy (EDS) and Light Yield (LY) characterisation to put into evidence possible correlations between the samples microstructure and their mechanical and scintillation properties. In this paper we analysed the same samples on which Scalise et al. have already measured the Ultimate Tensile Strength (UTS) and Young Modulus (YM) [35]. Two samples among the five investigated samples were also submitted to a thermal annealing treatment at 300 °C for 10 h to study possible modifications of their microstructure and consequently of their mechanical and optical behaviour.

The main results obtained can be summarised as follows:

- the crystallographic structure of the samples is monoclinic, space group C2/C with lattice parameters $a=14.245(2)$ Å, $b=6.635(1)$ Å, $c=10.242(1)$ Å, $\beta=122.188(10)^\circ$ and a crystal cell volume $V=819.26(18)$ Å^3;
- SEM observations did not evidence any defect nor any element segregation or compound formation on the crystals surface;
- EDS analyses carried out in conjunction with the SEM observations evidenced variations in the Lu (ranging from 22.8 at% to 28.9 at%), Y (ranging from 2.5 at% to 3.0 at%) and Ce (<1 at%) content of the samples;
- the values of UTS and YM measured for the different samples are not correlated with the variations of their mean chemical composition;
- TEM observations found that the sample with the lowest values of UTS and YM (sample 6, submitted to the annealing treatment) shows a non-homogeneous distribution of coherent spherical particles with size ranging from 10 to 15 nm;
- EDS analyses performed in conjunction with the TEM observations evidenced an increase of the Lu and Y content in correspondence of the coherent spherical particles with respect to the matrix;
- the LY response of the different samples is very similar regardless the thermal treatment undergone and the sample microstructure.

The results obtained in this work allow to conclude that the variations of the average chemical composition experimentally measured do not affect both the scintillation response and the mechanical behaviour of the analysed crystals. On the contrary, the presence of extended lattice defects in the form of spherical coherent particles inside the crystal strongly reduces the UTS and YM values. Finally, although the annealing temperature (300 °C) used in the heat treatment of the samples could induce the formation of the coherent lattice defects that strongly affect the mechanical response of the crystals, it is however not sufficiently high to induce annealing of the oxygen vacancies traps that are responsible of the deterioration of the scintillation properties of the LYSO:Ce crystals.

In order to better understand the mechanisms involved in the formation of the coherent lattice defects and to develop a theoretical model able to justify the mechanical response of the crystals in presence of extended lattice defects, further investigations are in progress.

Acknowledgements

This study was carried out in the framework of the Crystal Clear Collaboration (CCC).

References

[1] C.L. Melcher, J.S. Schweitzer, IEEE Transactions on Nuclear Science NS 39 (1992) 502.
[2] C.L. Melcher, Nuclear Instruments and Methods in Physics Resesearch A 537 (2005) 6.
[3] M. Nikl, Measurement Science and Technology 17 (2006) R37.
[4] P. Lecoq, A. Annenkov, A. Gektin, M. Korzhik, C. Pedrini, Inorganic Scintillators for Detector Systems, Springer, The Netherlands, 2006.

[5] J. Chen, L. Zhang, R. Zhu, Nuclear Instruments and Methods in Physics Research A 572 (2007) 218.
[6] B.D. Milbrath, A.J. Peurrung, M. Bliss, W.J. Weber, Journal of Materials Research 23 (2008) 2561.
[7] C. Wanarak, W. Chewpraditkul, A. Phunpueok, Procedia Engineering 32 (2012) 765.
[8] E. Kim, M. Lee, T. Inoue, W. Wong, Clinical PET and PET/CT: Principles and Applications, Springer, The Netherlands (2013) 41.
[9] I.G. Valais, I.S. Kandarakis, A. Konstantinidis, D.N. Nikolopoulos, I. Sianoudis, D.A. Cavouras, N. Dimitropoulos, C.D. Nomicos, G.S. Panayiotakis, Nuclear Instruments and Methods in Physics Research A 569 (2006) 201.
[10] M. Korzhik, A. Fedorov, A. Annenkov, A. Borissevitch, A. Dossovitski, O. Missevitch, P. Lecoq, Nuclear Instruments and Methods in Physics Research A 571 (2007) 122.
[11] L. Eriksson, D. Townsend, M. Eriksson, C. Melcher, M. Schmand, B. Bendriem, R. Nutt, Nuclear Instruments and Methods in Physics Research A 525 (2004) 242.
[12] C.L. Melcher, The Journal of Nuclear Medicine 41 (2000) 1051.
[13] W.W. Moses, Nuclear Instruments and Methods in Physics Research A 580 (2007) 919.
[14] D. Chiriu, N. Faedda, A. Geddo Lehmann, P.C. Ricci, A. Anedda, S. Desgreniers, E. Fortin, Physical Review B 76 (2007) 054112.
[15] N.I. Leonyuk, E.L. Belokoneva, G. Bocelli, L. Righi, E.V. Shvanskii, R.V. Henrykhson, N.V. Kulman, D.E. Kozhbakhteeva, Journal of Crystal Growth 205 (1999) 361.
[16] T. Gustafsson, M. Klintenberg, S.E. Derenzo, M.J. Weber, J.O. Thomas, Acta Crystallographica C 57 (2001) 668.
[17] H. Cong, H. Zhang, J. Wang, W. Yu, J. Fan, X. Cheng, S. Sun, J. Zhang, Q. Lu, C. Jiang, R.I. Boughton, Journal of Applied Crystallography 42 (2009) 284.
[18] D. Ding, L. Weng, J. Yang, G. Ren, Y. Wu, Journal of Solid State Chemistry 209 (2014) 56.
[19] D. Ding, B. Liu, Y. Wu, J. Yang, G. Ren, J. Chen, Journal of Luminescence 154 (2014) 260.
[20] B.D. Milbrath, A.J. Peurrung, M. Bliss, W.J. Weber, Journal of Materials Research 23 (2008) 2561.
[21] M. Nikl, V.V. Laguta, A. Vedda, Physica Status Solidi B 245 (2008) 1701.
[22] S. Blahuta, A. Bessière, B. Viana, V. Ouspenski, E. Mattmann, J. Lejay, D. Gourier, Materials 4 (2011) 1224.
[23] L. Pidol, A. Kahn-Harari, B. Viana, E. Virey, B. Ferrand, P. Dorenbos, J.T.M. de Haas, C.W.E. van Eijk, IEEE Transactions on Nuclear Science NS 51 (2004) 1084.
[24] W. Chewpraditkul, L. Swiderski, M. Moszynski, T. Szczesniak, A. Syntfeld-Kazuch, C. Wanarak, P. Limsuwan, IEEE Transactions on Nuclear Science NS 56 (2009) 3800.
[25] W. Chewpraditkul, C. Wanarak, T. Szczesniak, M. Moszynski, Nuclear Instruments and Methods in Physics Research B 326 (2014) 103.
[26] S. Blahuta, A. Bessière, B. Viana, P. Dorenbos, V. Ouspenski, IEEE Transactions on Nuclear Science NS 60 (2013) 3134.
[27] H. Loudyi, Y. Guyot, J.C. Gacon, C. Pedrini, M.F. Joubert, Optical Materials 30 (2007) 26.
[28] L. Pidol, B. Viana, A. Kahn-Harari, B. Ferrand, P. Dorenbos, C.W.E. Van Eijk, Nuclear Instruments and Methods in Physics Research A 537 (2005) 256.
[29] A. Vedda, M. Nikl, M. Fasoli, E. Mihokova, J. Pejchal, M. Dusek, G. Ren, C.R. Stanek, K.J. McClellan, D.D. Byler, Physical Review B 78 (2008) 195123.
[30] D. Kurtsev, O. Sidletskiy, S. Neicheva, V. Bondar, O. Zelenskaya, V. Tarasov, M. Biatov, A. Gektin, Materials Research Bulletin 52 (2014) 25.
[31] M. Tyagi, F. Meng, M. Koschan, S.B. Donnald, H. Rothfuss, C.L. Melcher, Journal Physics D: Applied Physics 46 (2013) 475302.
[32] M.A. Spurrier, P. Szupryczynski, H. Rothfuss, K. Yang, A.A. Carey, C.L. Melcher, Journal of Crystal Growth 310 (2008) 2110.
[33] K. Yang, C.L. Melcher, M.A. Koschan, M. Zhuravleva, IEEE Transactions on Nuclear Science NS 58 (2011) 1394.
[34] M. Koschan, K. Yang, M. Zhuravleva, C.L. Melcher, Journal of Crystal Growth 352 (2012) 133.
[35] L. Scalise, D. Rinaldi, F. Davì, N. Paone, Nuclear Instruments and Methods in Physics Research A 654 (2011) 122.
[36] F. Davì, D. Rinaldi, IEEE Transactions on Nuclear Science NS 59 (2012) 2106.
[37] K. Schwartz, A.E. Volkov, M.V. Sorokin, R. Neumann, C. Trautmann, Physical Review B 82 (2010) 144116.
[38] A. Dauletbekova, J. Maniks, I. Manika, R. Zabels, A.T. Aklibekov, M.V. Zdorovets, Y. Bikhert, K. Schwartz, Nuclear Instruments and Methods in Physics Research B 286 (2012) 56.
[39] FullProf Suite, ⟨https://www.ill.eu/sites/fullprof/⟩.
[40] CASINO – monteCArlo SImulation of electroN trajectory in sOlids, ⟨http://www.gel.usherbrooke.ca/casino⟩.
[41] D. Ding, J. Yang, G. Ren, M. Nikl, S. Wang, Y. Wu, Z. Mao, Physica Status Solidi B 251 (2014) 1202.
[42] P. Hirsch, A. Howie, R.B. Nicholson, D.W. Pashley, M.J. Whelan, Electron Microscopy of Thin Crystals, R.E. Krieger Publishing Company, Malabar, Florida, 1977.